

Ozone Generation in the 214-nm Photolysis of Oxygen at 25 °C

A. Horowitz,¹ G. von Helden, W. Schneider, F. G. Simon, P. J. Crutzen, and G. K. Moortgat*

Air Chemistry Division, Max Planck Institut fur Chemie, D6500, Mainz, FRG (Received: December 28, 1987)

Ozone formation in the 214-nm photolysis of oxygen at pressures ranging from 380 to 1300 Torr was investigated. The rates of ozone formation increase with the square of oxygen pressure mirroring the pressure dependence of the absorption cross sections of oxygen. This observation demonstrates the importance of the collision-induced changes in oxygen absorbance and points to a need to examine the role of oxygen dimer (O_2)₂ in reactions initiated by its photodissociation. Because of the high dilution of ozone, its formation was found to be linear with time even though, on the average, its rate of photolysis exceeded the rate of its generation from oxygen. The quantum yield of ozone formation was 1.86 ± 0.17 independent of O_2 pressure. From this result the quantum yield of the primary process $O_2 + h\nu$ (214 nm) $\rightarrow 2O(^3P)$ is estimated as being equal to 0.93 ± 0.08 (2σ). Based on the observed linear buildup of ozone and on model calculations, an upper limit of about 0.03 is estimated for O_3 photolysis via a channel which leads to $O(^3P)$ and an excited O_2 species that can regenerate ozone in its reaction with oxygen.

Introduction

The importance of ozone in the chemistry of air pollution and its vital role in attenuating solar UV radiation as well as fundamental interest in its photochemistry led to extensive studies which have been recently reviewed by the World Meteorological Organization² and by Wayne.³ In particular the understanding of the processes that govern the photochemical behavior of ozone and oxygen is of major importance for the precise assessment of the chemistry of the atmospheric ozone layer. In this layer the two most important processes are photodissociation of ozone as a result of light absorption in the Hartley band (200–360 nm) and photodissociation of molecular oxygen which follows light absorption in the Herzberg continuum (187–242 nm) corresponding to the forbidden $A^3\Sigma_u^+ \leftarrow X^3\Sigma_g^-$ transition.

Within most of the Hartley band the absorbed energy exceeds the threshold required for ozone dissociation into $O(^1D)$ and $O_2(^1\Delta_g)$ which onsets at about 310 nm. Indeed, below 310 nm this reaction was found to be the major photodissociation channel with quantum yields approaching unity.^{4–18} However, dissociation of ozone resulting in the formation of $O(^3P)$, characteristic of its photodecomposition at longer wavelength, is not suppressed completely even at 248 nm.^{16–18} The quantum yield of $O(^3P)$ formed via this route is about 0.1.

In view of the imbalance observed in the stratospheric ozone budget^{2,19,20} it is rather unfortunate that ozone photochemistry below 248 nm has not been extensively studied as at the longer wavelengths. The findings of the early studies of ozone photolysis at 228.8 nm by Lissi and Heicklen⁷ as well as those of Fairchild and Lee¹⁰ and Kajimoto and Cvetanovic,¹¹ who investigated ozone photolysis down to 230 nm, do not seem to rule out the possibility that, with the increase in the available energy, ozone photodissociation might occur along additional pathways. Conceivably, reactions of oxygen, with species formed via these additional photodissociation channels, could result in an enhanced regeneration of ozone and thus could constitute an additional source of "odd" oxygen in the stratosphere.²¹ This attractive possibility has not been investigated so far.

Finally, it is worth noting that, in all atmospheric model calculations related to ozone formation and destruction, the quantum yield of O_2 photodissociation in the Herzberg continuum is assumed to be unity. This is a very sound postulate which does not appear however to be based on a direct determination.

The present study of oxygen photolysis at 214 nm addresses itself to some of the problems related to the ozone balance in the atmosphere. In particular we were interested in the determination of the quantum yields of ozone formation under conditions where its secondary reactions can be minimized, i.e., when oxygen is present in large excess.

Experimental Section

Materials. Oxygen (Linde 5R) with a stated purity of 99.999% and water content of ≤ 3 ppm was used as received. Dew point measurements have shown that its actual moisture content was ≤ 0.3 ppm. Nitrosyl chloride (Matheson) was thoroughly degassed before its use.

Apparatus and Procedures. The steady-state photolysis of oxygen was carried out in a quartz shaped flushable cell that has been previously used in O_3 photolysis studies.⁸ The cell was mounted in an electrically heated aluminum block and connected to a greaseless vacuum system. O_2 pressures were measured with a Barocel electronic manometer and its moisture content, at the exit of the cell, was measured with a dew point moisture analyzer (Panametrics) capable of measuring dew points down to -80 °C (corresponding to 0.3 ppm at 1300 Torr).

The photolytic light source was a custom made 1-kW Sb lamp (Hereaus) from which the wavelength band centered near 214 nm was isolated by a combination of a 100-mm-long water filter cell and a 3-mm interference filter (Schott-UV-M-AL-214). The spectrum of the photolytic light is shown in Figure 1; its maximum is at 220 nm. However, O_2 absorption from this source, shown

- (1) Permanent address: Soreq Nuclear Research Center, Yavne, Israel.
- (2) World Meteorological Organization. "Atmospheric Ozone 1985. Global Research and Monitoring Project", 1986, Report No. 16.
- (3) Wayne, R. P. *Atmos. Environ.* **1987**, *21*, 1987.
- (4) DeMore, W. B.; Raper, O. F. *J. Chem. Phys.* **1966**, *44*, 1780.
- (5) Jones, I. T. N.; Wayne, R. P. *Proc. R. Soc. London Ser. A* **1971**, *321*, 409.
- (6) Wayne, R. P. *Faraday Discuss. Chem. Soc.* **1972**, *172*, 53.
- (7) Lissi, E.; Heicklen, J. *J. Photochem.* **1972**, *1*, 39.
- (8) (a) Moortgat, G. K.; Warneck, P. *Z. Naturforsch.* **1975**, *30a*, 835. (b) Arnold, J.; Comes, F. J.; Moortgat, K. G. *Chem. Phys.* **1977**, *24*, 211. (c) Moortgat, G. K. In *Proceedings of NATO Advanced Study Institute on Atmospheric Ozone: Its Variations and Influences, Algarve 1979*; U.S. Department of Transportation: Washington, DC, 1980; FAA-EE-80-20, p 559.
- (9) Amimoto, S. T.; Force, A. P.; Wiesenfeld, J. R. *Chem. Phys. Lett.* **1978**, *60*, 40.
- (10) Fairchild, P. W.; Lee, E. K. *Chem. Phys. Lett.* **1978**, *60*, 36.
- (11) Kajimoto, O.; Cvetanovic, R. J. *Int. J. Chem. Kinet.* **1979**, *11*, 605.
- (12) Brock, J. C.; Watson, R. T. *Chem. Phys. Lett.* **1980**, *71*, 371.
- (13) Fairchild, C. E.; Stone, E. J.; Lawrence, G. M. *J. Chem. Phys.* **1978**, *69*, 3632.
- (14) Sparks, R. K.; Carlson, L. R.; Shobatake, K.; Kowalczyk, M. L.; Lee, Y. T. *J. Chem. Phys.* **1972**, *72*, 1401.
- (15) Cobos, C.; Castellano, E.; Schumacher, H. J. *J. Photochem.* **1983**, *21*, 291.
- (16) Amimoto, S. T.; Force, S. P.; Wiesenfeld, J. R.; Young, R. H. *J. Chem. Phys.* **1980**, *73*, 1244.
- (17) Wine, P. H.; Ravishankara, A. R. *J. Chem. Phys.* **1982**, *69*, 365.
- (18) Greenblatt, G. D.; Wiesenfeld, J. R. *J. Chem. Phys.* **1983**, *78*, 4924.
- (19) Crutzen, P. J.; Schmailzl, U. *Planet. Space Sci.* **1983**, *31*, 1009.
- (20) Nicolet, M.; Kennes, R. *Planet. Space Sci.* **1986**, *36*, 1043.
- (21) (a) Saxon, R. P.; Slinger, T. G. *J. Geophys. Res.* **1986**, *91*, 9877. (b) Crutzen, P. In *Proceedings in the CMA Sponsored Meeting on Stratospheric Chemistry, Boulder, 1986*; Chemical Manufacturers Association: Washington, DC, 1986; CMA-FPP-85-559, p 157.

* To whom correspondence should be addressed.

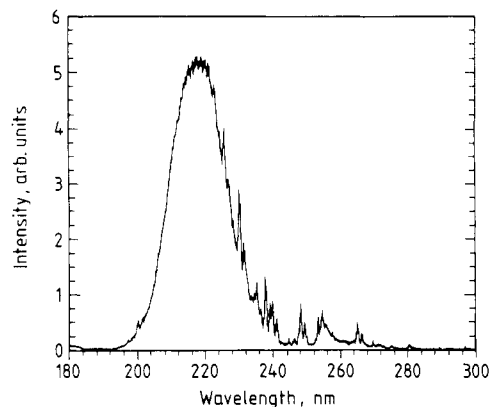


Figure 1. Spectrum of the photolytic light (1-kW Sb lamp + 100-mm H₂O filter + 214-nm interference filter).

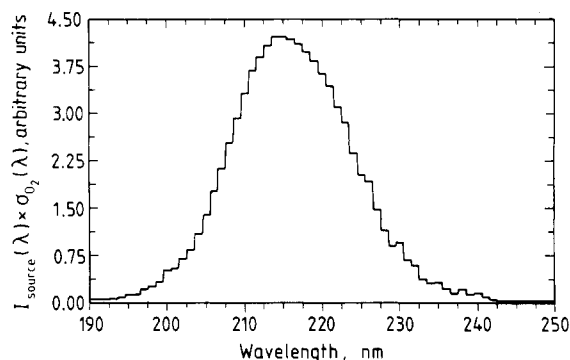


Figure 2. Effective oxygen absorption spectrum from the photolytic irradiation source at 1300 Torr.

in Figure 2, peaks at 214 nm. The intensity of the photolytic beam was monitored by a UV optimized silicon photodiode (Centronic OSD100-1) operating in a photovoltaic mode and connected to a picoammeter (Keithley 485) and from it, via an analog output, to a three-pen recorder. The optical path along the axis of the cell at which the photolysis was carried out was 11.6 cm. Similar arrangement was used to monitor ozone absorbance of 254-nm light generated by a low-pressure Hg lamp (Oriel 6035) along a 10-cm path perpendicular to the photolytic light and taking $\sigma_{O_3}(254) = 1.155 \times 10^{-17} \text{ cm}^2 \text{ molecule}^{-1}$.²² In order to prevent photolysis of ozone by the analytical light it was attenuated by passing it through two narrow iris diaphragm apertures and a 20% transmittance neutral-density filter. In this case the photodiode was screened from light at other wavelengths by a 254-nm interference filter mounted at its front. The neutral-density filter served also as a beam splitter thus allowing the monitoring of the intensity of the analytical beam. The signals from the three monitoring photodiodes were recorded simultaneously. Decomposition of ClNO, monitored at 254 nm and taking $\sigma_{ClNO}(254)^{23} = 2.37 \times 10^{-19} \text{ cm}^2 \text{ molecule}^{-1}$, was used for actinometry assuming that the quantum yield of its photodissociation equals to unity.²⁴ The amount of light absorbed by oxygen and ozone was estimated by integration of the product $\sigma(\lambda) \cdot I(\lambda) \cdot d\lambda$. In preliminary experiments, irreproducibility of the rates of ozone formation as a result of wall reactions was observed. The solution to this problem was found in a prolonged conditioning procedure which included baking and pumping of the cell at 100 °C followed by an overnight photolysis at this temperature of 1300 Torr of O₂.

Results

The formation of ozone was determined at several O₂ pressures ranging from 380 to 1300 Torr and as a function of incident light

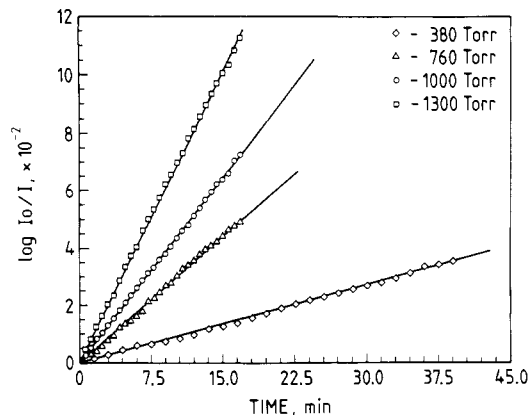


Figure 3. Buildup of ozone absorbance at 254 nm.

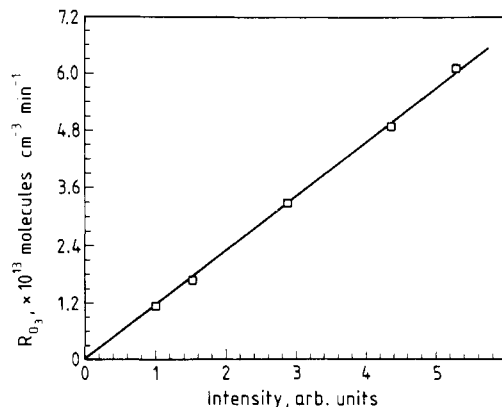


Figure 4. Variation of the rate of ozone formation with incident light intensity, O₂ = 1300 Torr.

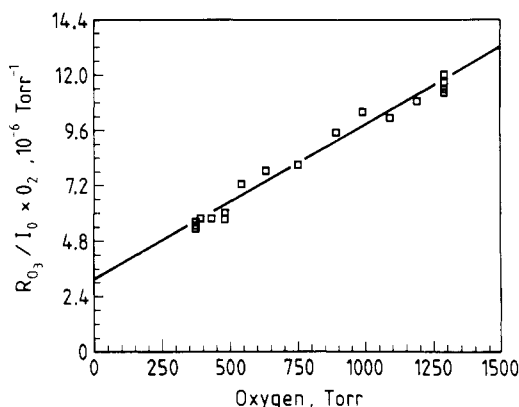


Figure 5. Plot of R_{O_3}/P_{O_2} vs P_{O_2} .

intensity. At the small conversions at which ozone formation was studied, no departure from linear variation of its concentration with time was observed, see Figure 3, although on average O₃ absorbed considerably more light than the oxygen. As expected, rates of ozone formation, R_{O_3} , were found to be proportional to the light intensity as shown in Figure 4. Rather unexpectedly though, an increase of R_{O_3} with the square of O₂ was observed. This effect is clearly demonstrated in the plot shown in Figure 5.

The effect of moisture was examined in a few runs in which the water content of the oxygen was about 2 ppm. This concentration did not remain constant throughout the runs because during each run some of the water was absorbed on the previously dried walls of the cell. Within experimental error, ozone formation was not affected by the presence of these amounts of water. The results of these experiments, together with those obtained at low moisture levels (H₂O ≤ 0.3 ppm), are presented in Table I.

Because of the previously discussed problems caused by surface reactions, experiments at 1300 Torr were conducted periodically

(22) Molina, L. T.; Molina, M. J. *J. Geophys. Res.* **1986**, *91*, 14501.

(23) Tyndall, G. S.; Stedman, K. M.; Schneider, W.; Burrows, J. P.; Moortgat, G. K. *J. Photochem.* **1987**, *36*, 133.

(24) (a) Kistiakowski, G. B. *J. Am. Chem. Soc.* **1930**, *52*, 102. (b) Wayne, R. P. *Nature* **1964**, *203*, 516.

TABLE I: Rate and Quantum Yield Data for Oxygen Photolysis at 214 nm^a

O ₂ , ^b Torr	time, s	I ₀ ^a × 10 ¹³ , quanta cm ⁻² s ⁻¹	I _{abs} / I ₀ × 10 ⁻³	R _{O₃} ^c × 10 ¹¹	R _{O₃'} ^c × 10 ¹¹	Φ _{O₃}	Φ _{O₃'}	O ₂ / O ₃ (final) × 10 ⁴	I _{abs} (O ₃)/ I _{abs} (O ₂)
380	2342	6.472	1.144	1.155	1.309	1.56	1.768	4.56	5.76
380	2160	6.403	1.144	1.210	1.356	1.652	1.851	4.71	5.58
380	2340	6.853	1.144	1.312	1.467	1.673	1.871	4.04	6.77
400	2160	6.583	1.232	1.373	1.520	1.693	1.874	4.37	5.88
440	1980	6.869	1.417	1.597	1.745	1.641	1.793	4.51	5.44
490	1980	6.350	1.664	1.655	1.792	1.567	1.696	4.85	4.81
490	1800	6.271	1.664	1.693	1.843	1.642	1.788	5.21	4.54
550	1440	7.054	1.984	2.677	2.824	1.913	2.018	5.38	4.85
640	1152	7.080	2.512	3.396	3.551	1.910	1.997	5.30	3.80
760	1008	6.763	3.304	4.019	4.175	1.799	1.868	6.08	2.99
900	1008	6.826	4.356	5.670	5.829	1.906	1.960	5.11	3.19
1000	1008	6.546	5.913	6.645	6.805	1.955	2.002	4.84	3.14
1100	1008	6.694	6.099	7.310	7.469	1.790	1.829	4.84	2.95
1200	1108	6.620	7.075	8.459	8.621	1.806	1.841	4.56	2.94
1300	1008	6.578	8.123	9.434	9.597	1.766	1.796	4.44	2.84
1300	1108	6.429	8.123	9.284	9.446	1.778	1.809	4.50	2.81
1300	1008	7.080	8.123	10.52	10.68	1.829	1.857	3.97	3.19
1300	1008	6.678	8.123	10.27	10.43	1.893	1.922	4.07	3.11
1300	1008	6.498	8.123	9.695	9.840	1.837	1.864	4.31	2.93
1300	1008	6.350	8.123	9.500	9.642	1.842	1.869	4.40	2.88

^a Rates in units of molecules cm⁻² s⁻¹. ^b Italicized pressures from experiments with ca. 2 ppm of water; in other experiments H₂O < 0.3 ppm. ^c R_{O₃} and R_{O₃'} observed and corrected for dark reaction, respectively.

between every two or three runs at the other pressures. As can be seen from the results presented in Table I, the reproducibility in these runs was quite satisfactory. However, even under the best experimental conditions, a dark reaction resulting in the loss of ozone, presumably at the cell walls, was observed and necessitated an appropriate correction of the R_{O₃} values. This correction amounts to about 13.5% at the lowest O₂ pressure of 380 Torr and it progressively decreases with this pressure, as the dark reaction loss of O₃ becomes relatively small as compared to its rate of formation. At the highest O₂ pressure the correction amounted to 1.5% only.

Discussion

The Role of Oxygen Dimer. In principle, the observed increase of the rates of ozone formation with the square of oxygen pressure can be attributed either to some unknown photochemical and photophysical processes that result in an increase of Φ_{O₃} or to nonlinear effect in the absorption of O₂ in the Herzberg continuum. Our choice of the latter alternative is based on the fact that an increase of O₂ absorption cross section with increasing oxygen pressure indeed has been observed and is well documented.²⁵⁻²⁸ This assumption is further supported by the observation that linear least-squares fit of the data plotted in Figure 5 gives R_{O₃}/P_{O₂}I₀ = (3.09 ± 0.40) × 10⁻⁶ + (6.60 ± 0.43) × 10⁻⁹P_{O₂}. The slope to intercept ratio obtained from this relation of (2.14 ± 0.31) × 10⁻³ Torr⁻¹ compares very well the slope/intercept ratio derived from the results of Cheung et al.²⁵ or the pressure dependence of the absorption cross section of O₂, σ_{O₂}, in the pressure range 5-760 Torr. These authors used the following expression for the pressure dependence

$$\sigma_{O_2}(\lambda) = \sigma_O(\lambda) + \alpha(\lambda)P_{O_2} \quad (1)$$

where P_{O₂} is in Torr and σ_O(λ) is the pressure-independent absorption cross section. They found, at 296-300 K, that α(λ)/σ_O(λ) = (2.05 ± 0.17) × 10⁻³, (2.00 ± 0.18) × 10⁻³, and (2.13 ± 0.24) × 10⁻³ Torr⁻¹ at 210, 215, and 220 nm, respectively. The agreement with the results of Johnston²⁶ is also quite good. In this case σ_{O₂} was measured at 297 K and pressures ranging from 100 to 760 Torr. The slope/intercept ratios, obtained for the same wavelengths as before, derived from their results are (1.74 ± 0.17)

× 10⁻³, (2.34 ± 0.23) × 10⁻³, and (1.80 ± 0.21) × 10⁻³ Torr⁻¹. Our results cannot be compared however to the findings of Shardanand and Rao²⁷ because their study was conducted mainly at high pressures, from 1 to 25 atm. The extended pressure range allows, in this case, a very precise determination of the pressure sensitive term, at the same time, as a result of insufficient low-pressure data, it yields very inaccurate intercept values.

The pressure dependence of oxygen absorption cross sections in the Herzberg continuum is usually ascribed in the absorbance of the weakly bound dimer, (O₂)₂ or O₄, which is in an equilibrium with oxygen, reaction 2. Accordingly, the pressure-dependent



term in eq 1, can be considered as being equal to K₂σ_{(O₂)₂}P_{O₂}. Using the detailed spectral data for O₂ of Cheung et al.²⁵ and integrating it over the spectrum of the photolysing light, given in Figure 1, it can be shown that 45% of the light absorbed at O₂ pressure of 380 Torr is due to (O₂)₂ absorption. Furthermore, for most of the pressures employed, the dimer absorbs over half of the absorbed light and this fraction reaches 75% at 1300 Torr. Hence, before any conclusion can be drawn from the present results, the possible consequences of this observation, which, to a large extent depend on the photochemical behavior of the O₂ dimer and the nature of its bonding, have to be examined.

Absorption of oxygen in the near-UV, the visible, and the infrared is known for more than a century. The early studies have been recently discussed by Platt and Perner²⁹ in the context of their measurements of the 300-350 nm absorbance of (O₂)₂ in the atmosphere and its chemical consequences. It appears however, that inasmuch as the nature of the bonding in (O₂)₂ is concerned, the most informative work is the study by Long and Ewing in which the infrared absorption of gaseous O₂ from 1480 to 1800 cm⁻¹ and between 77 and 300 K was examined.³⁰ These authors observed in the O₂ absorption spectrum a structureless band down to 90 K, where a doublet appears. Absorption in both regions increased with the square of O₂ concentration and hence Long and Ewing rationalized their findings in terms of two distinct phenomena: collision-induced absorption resulting in structureless bands, and formation at low temperatures of an (O₂)₂ bound by van der Waals interactions. For the latter species they estimated, from the temperature dependence of the doublet absorption, an activation energy of formation equal to 530 cal mol⁻¹. The corresponding value for the temperature dependence of the collision-induced spectrum was found to be lower by more than an

(25) Cheung, A. S. C.; Yoshino, K. Y.; Parkinson, W. H.; Guberman, S. L.; Freeman, D. E. *Planet. Space Sci.* **1986**, *34*, 1007.

(26) Johnston, H. S.; Paige, M.; Yao, F. *J. Geophys. Res.* **1984**, *89*, 11661.

(27) Shardanand; Prasad Rao, A. D. *J. Quant. Spectrosc. Radiat. Transfer* **1977**, *17*, 433.

(28) Jenouvrier, A.; Coquart, B.; Merienne-Lofar, *Planet. Space Sci.* **1986**, *34*, 253.

(29) Perner, D.; Platt, U. *Geophys. Res. Lett.* **1980**, *7*, 1053.

(30) Long, C. A.; Ewing, G. E. *Chem. Phys. Lett.* **1971**, *9*, 225.

order of magnitude. Johnston et al.²⁶ also arrived at a similar conclusion. They determined O₂ cross sections in the Herzberg continuum from 206 to 327 K. Johnston et al. derived the temperature dependence of K₂ from the macroscopic virial coefficient B, given by eq 3, and the excluded volume b in the microscopic equation of state, eq 4; where n₂ and n₄ are the molar concen-

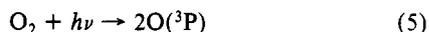
$$PV/nRT = 1 + nB/V + \dots \quad (3)$$

$$P(V - b) = (n_2 + n_4)RT \quad (4)$$

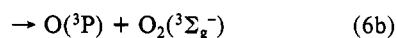
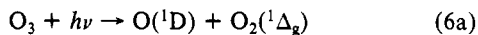
trations of oxygen and its dimer, respectively. The values of K₂ thus obtained increased by a factor of about 2 from 327 to 206 K, in marked contrast to the experimental findings that, within experimental error, the term reflecting (O₂)₂ absorbance did not show any detectable variation with temperature. On the basis of this observation and the parallelism between the O₂ and (O₂)₂ spectra these authors concluded that the pressure dependence of O₂ spectrum is caused by a perturbation of the wave function of an oxygen molecule by the force field of nearby O₂ rather than by stable dimer formation.

Our results appear to be a first demonstration of the correspondence between the pressure dependence of O₂ absorption in the Herzberg continuum and its photochemistry. Nevertheless, in view of the rather convincing evidence, we tend to accept the opinion that (O₂)₂ and O₄ reflect a convenient notation more than an existence of a real species that could differ from molecular oxygen in its primary photodissociation processes. In other words, we shall assume that O₂ and O₄ photodissociation processes are kinetically indistinguishable.

Mechanism and Quantum Yields. Based on the conclusion reached in the previous section and the observation of Lee et al.³¹ that in the 170–237-nm region the quantum yield of the energetically possible dissociation channel leading to O(¹S) does not exceed 0.001, photodissociation of O₂ under our experimental conditions appears to be fully accounted for by reaction 5.



However, even in the present system in which the average O₂/O₃ concentration ratio was as high as $(2.35 \pm 0.5) \times 10^4$, photolysis of ozone could not be completely suppressed. It can be seen from the results presented in Table I, that, at the end of all runs, the amount of light absorbed by ozone considerably exceeded the amount absorbed by oxygen. The value of $I_{\text{abs}}(\text{O}_3)/I_{\text{abs}}(\text{O}_2)$ at the end of the runs was close to 3 at the highest pressure and about 6 at the lower one. Accordingly the following reactions have to be also considered



Subsequently, the initially formed species can react either with ozone or with oxygen according to the following reaction scheme:

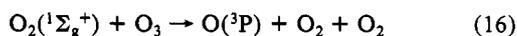
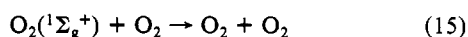
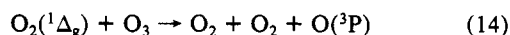
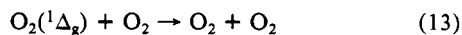
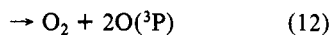
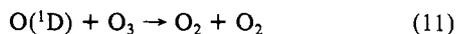
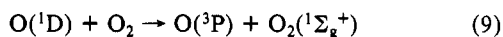
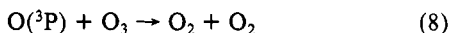
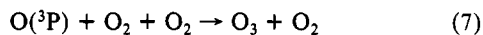
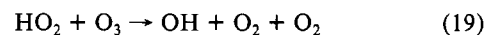
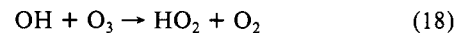
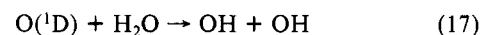


TABLE II: Summary of Photochemical Reactions Used in the Model Calculations of Oxygen Photolysis at 214 nm^a

reaction	rate constant ^b	ref and notes
O ₂ + hν → 2O(³ P)	1.0 × I _{abs}	25, c
O ₃ + hν → O(¹ D) + O ₂ (¹ Δ _g)	0.9 × I _{abs}	22, d
→ O(³ P) + O ₂	0.1 × I _{abs}	22
→ O(³ P) + O ₂ (A ³ Σ _u ⁺)	(0.03–0.10) × I _{abs}	22, e
H ₂ O ₂ + hν → 2OH	1.0 × I _{abs}	33
O(¹ D) + O ₂ → O(³ P) + O ₂ (¹ Σ _g ⁺)	2.0 × 10 ⁻¹¹	34, 35
→ O(³ P) + O ₂	2.0 × 10 ⁻¹¹	34, 35
O(¹ D) + O ₃ → O ₂ + 2O(³ P)	1.2 × 10 ⁻¹⁰	34
→ 2O ₂	1.2 × 10 ⁻¹⁰	34
O(¹ D) + H ₂ O → 2OH	2.2 × 10 ⁻¹⁰	36
→ O(³ P) + H ₂ O	1.2 × 10 ⁻¹¹	36
→ H ₂ + O ₂	2.3 × 10 ⁻¹²	36
O(¹ D) + H ₂ → OH + H	1.0 × 10 ⁻¹¹	34
O ₂ (¹ Δ _g) + O ₂ → 2O ₂	2.2 × 10 ⁻¹²	35
O ₂ (¹ Δ _g) + O ₃ → 2O ₂ + O(³ P)	3.8 × 10 ⁻¹⁵	35
O ₂ (¹ Δ _g) + H ₂ O → O ₂ + H ₂ O	5.0 × 10 ⁻¹³	35
O ₂ (¹ Δ _g) + O ₂ (¹ Δ _g) → O ₂ (¹ Σ _g ⁺) + O ₂	2.0 × 10 ⁻¹⁷	37
O ₂ (¹ Σ _g ⁺) + O ₂ → 2O ₂	4.0 × 10 ⁻¹⁷	36
O ₂ (¹ Σ _g ⁺) + O ₃ → 2O ₂ + O(³ P)	1.5 × 10 ⁻¹¹	36
→ O ₂ (¹ Δ _g) + O ₃	3.5 × 10 ⁻¹²	36
→ O ₂ + O ₃	3.5 × 10 ⁻¹²	36
O ₂ (¹ Σ _g ⁺) + H ₂ O → O ₂ + H ₂ O	6.0 × 10 ⁻¹²	36
O(³ P) + O ₃ → 2O ₂	8.0 × 10 ⁻¹⁵	34
O(³ P) + O ₂ + O ₂ → O ₃ + O	6.2 × 10 ⁻³⁴	36
O(³ P) + H ₂ O ₂ → OH + HO ₂	1.7 × 10 ⁻¹⁵	36
O(³ P) + H ₂ → OH + H	9.0 × 10 ⁻¹²	36
O(³ P) + HO ₂ → OH + O ₂	5.9 × 10 ⁻¹¹	34
O(³ P) + OH → O ₂ + H	3.3 × 10 ⁻¹¹	36
OH + O ₃ → HO ₂ + O ₂	6.8 × 10 ⁻¹⁴	34
OH + OH → H ₂ O + O(³ P)	1.8 × 10 ⁻¹²	36
OH + OH + O ₂ → H ₂ O ₂ + O ₂	6.9 × 10 ⁻³¹	36
OH + HO ₂ → H ₂ O + O ₂	7.0 × 10 ⁻¹¹	34
OH + HO ₂ + O ₂ → H ₂ O + 2O ₂	1.6 × 10 ⁻³¹	34
OH + H ₂ O ₂ → H ₂ O + HO ₂	1.7 × 10 ⁻¹²	34
OH + H ₂ → H ₂ O + H	6.7 × 10 ⁻¹⁵	34
HO ₂ + O ₃ → OH + O ₂	2.0 × 10 ⁻¹⁵	34
HO ₂ + HO ₂ → H ₂ O ₂ + O ₂	1.7 × 10 ⁻¹²	34
HO ₂ + HO ₂ + O ₂ → H ₂ O ₂ + O ₂	4.9 × 10 ⁻³²	34
H + O ₂ + O ₂ → HO ₂ + O ₂	5.9 × 10 ⁻³²	36
O ₂ (A ³ Σ _u ⁺) + O ₂ → O(³ P) + O ₂	2.9 × 10 ⁻¹³	32

^aI₀ = 6.75 × 10¹³ quanta cm⁻³ s⁻¹. ^bRate constants in units of cm³ molecule⁻¹ s⁻¹ and cm⁶ molecule⁻² s⁻¹ for bimolecular and termolecular reactions, respectively. ^cQuantum yield of unity assumed. ^dQuantum yields as discussed in text. ^eAssumed quantum yield of 0.03–0.1 at the expense of O(¹D) formation.

In terms of this reaction scheme it is quite clear (see Table II) that decomposition of ozone in its mixtures with oxygen will take place only if the amount of oxygen is not sufficient to suppress completely the reactions of O(¹D), O(³P), O₂(¹Δ_g), and O₂(¹Σ_g⁺) with ozone. The situation becomes more complex, however, when traces of water are present in the system. In this case, generation of the hydroxyl radical via reaction 17, can lead to a chain decomposition of ozone propagated mainly by reactions 18 and 19.



Decomposition of ozone should be indicated by a decrease in its rate of formation which in turn has to be reflected in the quantum yields, Φ_{O₃}, given in Table I and which were computed on the basis of the amount of light absorbed by oxygen. From our results we obtain Φ_{O₃} = 1.86 ± 0.17 (2σ) with no indication of pressure dependence, which would be expected to exist if the reaction of O(¹D) with water or ozone had taken place. Also, in line with this argument, the presence of small amounts of water did not affect the O₃ quantum yield and within the experimental error, no departure from linearity of ozone growth with time was detected. These observations seem to provide a strong support for the assumption that, under the experimental conditions in this work, O(¹D) atoms react only with oxygen. In this case, it can

(31) Lee, L. C.; Black, G.; Sharpless, R. L.; Slinger, T. G. *J. Chem. Phys.* 1980, 73, 256.

TABLE III: Model Computed Values of Ozone Formation in the 214-nm Photolysis of Oxygen^a

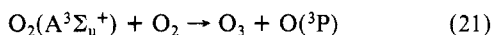
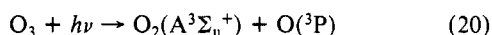
$O_2 \times 10^{19b}$	$H_2O \times 10^{13}$	$\Phi(A^3\Sigma_u^+)$	$O_{3,in} \times 10^{13c}$	$O_{3,f} \times 10^{13d}$
1.23	0	0	0.928	3.617 (3.617)
	3.7	0	0.928	3.598 (3.671)
	3.7	0.03	0.934	4.048 (3.642)
2.46	3.7	0.1	0.937	5.420 (3.654)
	0	0	2.677	4.498 (4.498)
	7.4	0	2.677	4.488 (4.498)
	7.4	0.03	2.687	4.720 (4.514)
4.21	7.4	0.1	2.709	5.325 (4.551)
	0	0	6.583	11.06 (11.06)
	12.6	0	6.583	11.06 (11.06)
	12.6	0.03	6.606	11.59 (11.10)
	12.6	0.1	6.662	13.08 (11.19)

^aAll concentrations in units of molecules cm^{-3} . ^bThe corresponding pressures in Torr are 380, 760 and 1300. ^cOzone concentrations after 60 s. ^dOzone concentrations after 2.34×10^3 , 1.08×10^3 , and 1.08×10^3 s at O_2 pressures of 380, 760, and 1300 Torr, respectively; in parentheses are ozone concentrations at the same times extrapolated linearly from the values at 60 s in previous column.

be inferred from our results that the primary quantum yield of oxygen photodissociation is close to unity.

As a final test of the accuracy and meaning of the quantum yields determined in this work, model calculations were carried out. In these calculations all possible reactions, in the dry as well as the water-containing systems, were included in order to examine any possible cause for nonlinearity of R_{O_3} and reduction of Φ_{O_3} . A complete list of the reactions included in the simulation and their rate constants is presented in Table II.

Potential formation of ozone in reactions 20 and 21 involving O_2 in the $A^3\Sigma_u^+$ state was also tested by the model calculations. We assumed conditions that would maximize ozone formation from this source, namely formation of $O_2(A^3\Sigma_u^+)$ at the expense of $O(^1D)$ and neglecting the possibility that the collision deactivation reaction 22 can also take place. In fact, only its overall rate constant was determined by Kenner and Ogryzlo.³²



Turning now to the results of the model calculations summarized in Table III, it should be emphasized that the simulation includes an assumption that the photodissociation of oxygen proceeds with a quantum yield of unity. Consequently, linearity with time of the rate of ozone formation should be considered as a confirmation of the procedures used in the experimental determination of ϕ_{-O_2} . It should also be mentioned that, as an additional precaution in the linearity test, the water concentration was set at 3 ppm, the upper limit specified by the manufacturer. This value is by an order of magnitude higher than the measured water content. It can be seen that, even under these rather extreme conditions, the maximum expected deviation from linearity at 380 Torr, is less than 1%. We conclude thus that ϕ_{-O_2} is indeed very close to unity as indicated by the experimentally determined value of 0.93 ± 0.08 (2σ), the error limits of which reflect the scatter of the results but do not take into account systematic errors. Inaccuracies in the absorption spectra of O_2 and O_3 appear to be the main causes of such errors.

(32) Kenner, R. D.; Ogryzlo, E. A. *Int. J. Chem. Kinet.* **1980**, *12*, 501.

The model calculations seem also to exclude the possibility that, under our experimental conditions, $O_2(A^3\Sigma_u^+)$ has a major role in the mechanism of ozone formation. Since within the experimental time scale the presence of water does not reduce the rate of ozone formation, the ozone-generating reactions of molecular oxygen in this state should result in an upward curvature in the time dependence of ozone build up. This assumption is indeed verified by the model calculations. However, even if as a measure of safety we assume that failure to detect 10% deviation from linearity was possible, the model calculations show that the quantum yield of the primary photodissociation step in which $O_2(A^3\Sigma_u^+)$ is formed cannot exceed 0.03.

Atmospheric Consequences. Since it is generally assumed that photodissociation of O_2 in the Herzberg continuum proceeds with a quantum yield of unity, the present results do not seem to have any direct bearing upon the known chemistry of ozone formation. Indirectly, however, we were able to show that, at least at 214 nm, $O_2(A^3\Sigma_u^+)$ cannot be an important source of ozone in the atmosphere. This conclusion applies to any other states of O_2 formed in the photolysis of ozone at 214 nm. The suggestion of Saxon and Slanger^{21a} and of Crutzen^{21b} that the A and A' states, potentially formed upon ozone photolysis below 230 nm, could generate significant amounts of ozone in their reactions with ground-state oxygen thus does not seem to be borne out by the experimental findings at high O_2 pressures. Conceivably, such reactions could become important at lower pressures and shorter wavelength. This possibility is presently investigated by us. At the same time, the present results do not exclude the possibility that A and A' excited oxygen molecules, formed by recombination of atomic O



generate ozone in their reaction with O_2 . This mechanism of ozone formation at altitudes of ca. 100 km was suggested by Allen.³⁸ However, it could not be tested at the high O_2 pressures employed by us where O atoms are predominantly removed by first-order reactions as indicated by the observed linear variation of the rate of ozone formation with incident light intensity, shown in Figure 4.

The clear demonstration that O_2 - O_2 interactions are reflected in the photodissociation of oxygen is quite important in as far as extrapolation of laboratory results to the real atmosphere is concerned. For instance, a rather trivial error can occur when pressure effects on various reactions initiated by O_2 photodissociation are investigated and the experimental results are interpreted assuming a constant absorption cross section. Isotope enrichment studies represent another case where misinterpretation of the results is possible, in particular if the O_2 dimer exhibits isotope selectivity in its photodissociation reactions.

Acknowledgment. We thank T. G. Slanger (SRI) for helpful suggestions. A.H. gratefully acknowledges MPI Visiting Scientist Fellowship.

Registry No. O_3 , 10028-15-6; O_2 , 7782-44-7; O, 17778-80-2.

(33) "Chemical Kinetics and Photochemical Data for Use in Stratospheric Modeling"; NASA Evaluation No. 6, 1983, JPL 83-62.

(34) "Chemical Kinetics and Photochemical Data for Use in Stratospheric Modeling"; NASA Evaluation No. 7, 1985, JPL 85-37.

(35) "CODATA Evaluated Kinetic and Photochemical Data for Atmospheric Chemistry"; Suppl. No. 1. *J. Phys. Chem. Ref. Data* **1982**, *11*, 327.

(36) "CODATA Evaluated Kinetic and Photochemical Data for Atmospheric Chemistry"; Suppl. No. 2. *J. Phys. Chem. Ref. Data* **1984**, *13*, 1259.

(37) Fisk, G. A.; Hays, G. N. *J. Chem. Phys.* **1982**, *77*, 4965.

(38) Allen, M. J. *Geophys. Res.* **1986**, *91*, 2844.